

## H I MAPPING OF GALAXIES IN THE HERCULES CLUSTER

E. E. SALPETER

Center for Radiophysics and Space Research, Cornell University

AND

J. M. DICKEY

Astronomy Department, University of Minnesota

Received 1984 September 4; accepted 1984 December 4

### ABSTRACT

We have made an H I survey, using 32 frequency channels, with the VLA D-configuration, of three fields centered on the Hercules cluster of galaxies (A2151). We have detections (or possible detections) for 31 optically known galaxies, of which 13 are optically bright Zwicky galaxies. We have evidence for at most one H I source which is not associated with an optical galaxy. Our detections include three galaxy pairs which are unresolved to one Arecibo beam. One of these pairs contains the peculiar galaxy IC 1182 with a jet pointing toward the companion.

For 16 of the 31 detected galaxies the center position is different for the emission in different frequency channels, i.e., we have a rotation signature. There is no preferred direction in the sky for the principal axis of this signature. The core of A2151, although elongated and clumpy, is probably a single dynamic unit, and the dispersion of systemic velocities decreases with increasing distance from the cluster core. There is a small increase of systemic velocities from south to north (with an overall mean of  $10,957 \pm 114 \text{ km s}^{-1}$ ). Undetected spirals have a marginally larger mean optical velocity than other galaxies, but approximately the same dispersion of systemic velocities.

*Subject headings:* galaxies: clustering — radio sources: 21 cm radiation

### I. INTRODUCTION

The Hercules cluster of galaxies (A2151) is spiral-rich and “unrelaxed” (i.e., its core has an irregular density distribution) like the well-studied Virgo cluster, but its redshift is  $\sim 10$  times larger. For many comparative studies H I data are required, and the brightest spiral galaxies in the Hercules cluster (and its surroundings) have already been observed at Arecibo by various groups (Schommer, Sullivan, and Bothun 1981; Giovanelli, Chincarini, and Haynes 1981), and a recent compilation (Giovanelli and Haynes 1984) was kindly made available to us before publication (another Arecibo compilation will be contained in Bothun *et al.* 1985). Because of the large distance of the Hercules cluster, the Arecibo beam size of  $\sim 3'$  is much larger than even the brightest spirals (diameters  $< 1.5$ ), and there is some danger of blending of emission from more than one galaxy in a single Arecibo beam, especially for the crowded cluster core. For this reason we have carried out H I observations on three fields with the D-configuration of the VLA (NRAO),<sup>1</sup> covering most of the core of A2151. Besides resolving pairs, this study resolves a number of individual galaxies and gives the principal axis for the galaxy rotation. We also detect a number of optically faint, hydrogen-rich galaxies.

The core of A2151 is elongated, approximately in the N-S direction, and our three fields (see § II) contain 38 optically bright galaxies from field Z108 of Zwicky, for which optical redshifts were determined by Tarengi *et al.* (1979). A list of 120 galaxies (including the 38, which we shall call the T list) with morphological types is given by Dressler (1980; hereafter the D list). A list of even fainter galaxies, not on the D list and

not known to be ellipticals, with coordinates accurate to better than  $3''$ , was kindly made available to us prior to publication by Okamura and his colleagues. We denote this list (Okamura and Wakamatsu 1983) by OW; an expanded version of their catalog is expected for 1985. Our basic H I spectral maps (procedures described in § II) were searched for emission from each of these galaxies, and the results are presented in § III.

Since many of our data are only slightly above the detection threshold, we calibrate the internal error estimates by comparisons with Arecibo and optical data in § IV. The hydrogen content is discussed in § V and an interesting pair of “interacting” galaxies (including the peculiar galaxy IC 1182) in § VI. In § VII we discuss the distribution of systemic velocities and its relevance to dynamics, following a previous discussion by Tarengi *et al.* (1980).

### II. OBSERVATIONS AND REDUCTION

In principle, an aperture synthesis telescope like the VLA is particularly appropriate for observations of galaxies in clusters, because the primary beam covers a large fraction of the cluster area, so that in a single observation we can simultaneously map many galaxies. The problem with aperture synthesis arrays for observing galaxies is that they are usually sparsely filled, which means that their brightness sensitivity is poor. The typical brightness temperature of the H I emission from Hercules spirals is only a few tenths of a kelvin. To detect this emission requires many hours of integration, even with the D-array, which is the most filled aperture available among the major synthesis arrays in operation. Although the C-array would have given us much higher resolution, our sensitivity to arc minute size sources would be much less with the C-array.

The half-power beam half-width of the VLA primary at 21 cm wavelength is  $\sim 16'$ ; we have covered the richer portions of

<sup>1</sup> The NRAO is operated by Associated Universities, Inc., under contract with the National Science Foundation.

Hercules with three observations centered on the following positions:

- 1) Right ascension (1950) =  $16^{\text{h}}02^{\text{m}}40^{\text{s}}$ , declination (1950) =  $+17^{\circ}36'30''$ ;
- 2) Right ascension (1950) =  $16^{\text{h}}02^{\text{m}}40^{\text{s}}$ , declination (1950) =  $+17^{\circ}51'00''$ ;
- 3) Right ascension (1950) =  $16^{\text{h}}03^{\text{m}}45^{\text{s}}$ , declination (1950) =  $+18^{\circ}16'30''$ .

These fields were observed on 1983 June 28, 30, and July 1, for 10, 12, and 12 hr, respectively. The spectrometer channel width was set at  $781.25 \text{ kHz} = 175 \text{ km s}^{-1}$ , with a total bandwidth of 25 MHz. The band was centered on  $10,700 \text{ km s}^{-1}$  (the nominal Hercules redshift) for the first observation, but a serious interference spike at 1361.2 MHz caused us to move the center to  $10,000 \text{ km s}^{-1}$  for the second two observations. Flux calibration was done using 3C 48 and 3C 286; bandpass calibration was done using 1607 + 268. The standard VLA Dec-10 calibration and editing programs were used. Maps were made on the AIPS systems at the VLA and at the University of Minnesota. The continuum emission was subtracted from the line channel maps in three steps. First, the clean components of the final continuum maps were subtracted from the UV data of each spectral channel. Then the residuals of the continuum map (i.e., the dirty map minus the clean components convolved with the dirty beam) were subtracted from the line channel maps. Finally, the average of all  $n$  channels was subtracted from each map, and the resultant multiplied by  $(n + 1)/n$ ; this makes a further slight improvement in the rms noise. The final noise level on the line maps is  $\sim 600$  microjanskys per beam area, which corresponds to dynamic range of  $\sim 750$  relative to the continuum. These fluctuations are probably dominated by radiometer noise; they are within a factor of 2 of the theoretical noise level.

The final maps were not cleaned, because there are no sources stronger than  $\sim 10$  times the noise level. The best-fit Gaussian to the synthesized beam has axes  $42'' \times 40''$ , which is the resolution of the maps. The peak sidelobe level is  $\sim 3\%$ , as discussed by Hjellming (1983).

The spectral maps were assembled into a cube, which was studied both by taking moments (e.g., van Gorkum 1983) and by slicing to obtain spectra at the positions of known galaxies. When lines or suspected lines were found, we fitted two-dimensional Gaussians to the channel maps using the AIPS task IMFIT. It is the results from this process which are used below to compute hydrogen masses and rotation parameters for the galaxies detected.

### III. THE H I DATA

Although 32 frequency channels were used in the observations, only data from 26 channels were analyzed fully. Using the "optical definition" for Doppler velocity,  $V = (v_{\text{obs}}^{-1} v_{\text{rest}} - 1)c$ , the center velocity  $V_n$  (heliocentric) for the  $n$ th channel is close to

$$V_n = 12,674 - 179n + 0.1n^2 - 2.5 \times 10^{-5}n^4. \quad (1)$$

For each channel in each of the three fields we had a map with  $256 \times 256$  pixels with pixel spacing  $10''$ . The FWHP of the synthesized beam is about  $42'' \times 40''$ , and that of the primary beam is  $32.6$ . The gain factor, GF (the ratio of the primary on-center gain to that at the position of a galaxy) is given for each of the detected galaxies in Table 1 (if observed in more than one field, the smallest value of GF is given).

For each of the optical galaxies in the lists described in § I,

the radio frequency spectrum for the pixel nearest to the optical position was inspected visually. For any frequency channel showing an appreciable positive signal, as well as two channels on either side, a small map (about  $20 \times 20$  pixels) was inspected visually. If there was any possibility of a meaningful positive signal, the small map was analyzed by the AIPS "Gaussian Fit" program (IMFIT), once without any restrictions and once with the major and minor axes fixed to be  $42'' \times 40''$  FWHP. This program gives the central position and "typical errors"  $\sigma_{\text{RA}}$  and  $\sigma_{\text{dec}}$  in right ascension and declination, as well as an area-integrated channel flux  $F$  and "typical error"  $\sigma_F$  in this flux. The numerical value given by the AIPS program for  $\sigma_F$  was  $\sim 4$  or 5 times the rms noise fluctuations for any given pixel, presumably to account for the fact that the program searches the map for a "suitable center" and is thus sensitive to upward fluctuations in noise. Because of this search procedure the error distribution is not a "normal curve," since the Gaussian which controls very large excursions involves an rms of  $\sim 0.2 \sigma_F$  instead of  $\sigma_F$  in the exponent, where  $F$  and  $\sigma_F$  are in units of 0.1 mJy.

VLA fluxes are measured relative to known calibration sources which are chosen to be compact and unresolved. For a slightly extended source, the Gaussian fit with axes fixed at  $42'' \times 40''$  weights the central surface brightness more heavily than the area integral of the emission. When the signal to noise was poor, we had to use this procedure and thus systematically underestimated the total flux. When the signal was sufficiently strong, we relied mainly on the Gaussian model fit, with the principal axes allowed to vary. In such cases the fluxes  $F$  given in Table 1 are the area integrals of these models. However, if the actual emission has the form of a bright core plus a faint halo, this model fit is likely to miss the halo, in which case it again underestimates the total flux.

Table 1 gives data for individual frequency channels for all galaxies with a "possible H I detection." For each galaxy the first two lines give the galaxy number in the list by Dressler (1980), preceded by a "D," and the optical position (for galaxies not on this list the symbol "OW" denotes entries from the list by Okamura and Wakamatsu 1983). The criteria for inclusion of a galaxy were (a)  $F/\sigma_F > 1.5$  for at least one frequency channel, (b) only channels with  $F/\sigma_F > 1.0$  were included, (c) for at least one of the channels the center of the radio position lies within  $20''$  of the central optical position, and (d) only channels with center position within  $35''$  of the optical are included. A few cases of special interest, which do not satisfy these criteria, are added (in brackets) to Table 1. The rows (after the first two) for each galaxy give the frequency channel number, the displacement  $\Delta_{\text{RA}}$  (radio right ascension minus optical) with the error ( $\sigma_{\text{RA}}$ ) in the radio position, expressed in units of  $1 \text{ s} \approx 14.3$ , and the corresponding quantities  $\Delta_{\text{dec}}(\sigma)$  for declination, expressed in units of arc seconds.<sup>2</sup>

The AIPS Gaussian fit program gives values for the major and minor diameters (and position angle of the major diameter) for each assumed Gaussian. If these diameters are appreciably larger than the synthesized beam of  $42'' \times 40''$  (FWHP), the intrinsic size can be deconvolved from the beam. This was not possible unequivocally for the minor diameter in any of the cases, but we give the (approximately deconvolved) FWHP major diameter  $a$  at the right in Table 1 for all cases

<sup>2</sup> Positions of continuum sources are given in Table 1 of Dickey and Salpeter (1984). In that table, declinations for all sources from 42 through 66 should start with  $18^{\circ}$ .

TABLE 1  
 HI DATA FOR INDIVIDUAL FREQUENCY CHANNELS, REFERRED TO KNOWN OPTICAL GALAXIES

RA	x	Dec.	(Field)	GF	RA	x	Dec.	(Field)	GF
Ch	$F(\sigma_F)$	$\Delta RA (\sigma_{RA})$	$\Delta Dec(\sigma)$	size (",";";")	Ch	$F(\sigma_F)$	$\Delta RA (\sigma_{RA})$	$\Delta Dec(\sigma)$	size (",";";")
16 03	01.1	x 17 24 18	(1)	1.53	16 03	30.3	x 17 42 59	(1,2)	1.63
		[OW166]:					D38:		
9	19(12)	-0.1(1.0) <sub>x</sub>	+3(14)		2	22(11)	-1.8(0.8)	-16(14)	
10	19(18)	-4.3(1.4) <sub>x</sub>	+32(25)	(A)	3	34(13)	+0.2(0.7) <sub>x</sub>	0(10)	
10	20(23)	+0.1(1.8)	+23(36)	(B)					
10	19(18)	+0.5(1.3)	-41(29)	(C)	16 03	00.9	x 17 44 22	(1)	1.29
10	29(17)	+6.4(1.0)	+35(11)	(D)			[OW161]:		
16 03	31.6	x 17 26 28	(1)	2.0	11	23(15)	+0.9(1.1) <sub>x</sub>	+30(12)	
		D14:			16 02	52.0	x 17 47 02	(1,2)	1.06
10	54(33)	+0.6(1.2) <sub>x</sub>	-5(15)				D49:		
16 03	38.5	x 17 28 29	(1)	1.98	14	22(10)	-0.5(0.7) <sub>x</sub>	-14(13)	(52,0;15)
		D18:			16 02	13.7	x 17 47 03	(1,2)	1.15
13	26(16)	+1.1(1.4) <sub>x</sub>	+13(18)				D52:		
14	37(26)	+0.6(1.4) <sub>x</sub>	-20(18)		15	27(17)	+1.6(1.0) <sub>x</sub>	+7(18)	
16 02	32.1	x 17 28 58	(1)	1.16	16 03	11.4	x 17 49 54	(1,2)	1.15
		D20:					D60:		
11	26(10)	+0.3(0.7) <sub>x</sub>	-3(9)		8	33(11)	-0.4(0.6) <sub>x</sub>	+20(12)	
12	29(12)	+0.5(0.8) <sub>x</sub>	+10(11)		9	61(10)	+0.3(0.3) <sub>x</sub>	-5(5)	(23,0;140)
16 03	20.3	x 17 30 36	(1,2)	1.36	10	21(8)	+0.4(0.6)	-33(9)	
		[OW205]:			16 02	16.8	x 17 51 25	(1,2)	1.08
4	24(14)	-0.1(1.0) <sub>x</sub>	-14(18)				D66 (T101):		
16 02	57.0	x 17 33 25	(1,2)	1.06	19	15(10)	+0.6(1.2) <sub>x</sub>	+3(17)	
		D24 (T113):			16 03	07.3	x 17 52 39	(1,2)	1.12
11	14(12)	-1.6(1.3) <sub>x</sub>	-8(28)				[OW181]:		
12	35(09)	-1.0(0.5) <sub>x</sub>	-8(28)		25	18(9)	+0.3(0.8) <sub>x</sub>	-11(11)	
13	35(12)	+1.2(0.6) <sub>x</sub>	+21(7)		16 03	07.6	x 17 53 20	(1,2)	1.13
14	17(10)	+1.4(1.0)	+23(12)				D156 (T119W)		
16 02	04.0	x 17 34 19	(1,2)	1.20	8	12(8)	-0.6(1.0) <sub>x</sub>	+21(17)	
		D25:			9	51(8)	-0.1(0.3) <sub>x</sub>	-2(4)	
10	20(11)	+1.8(0.9) <sub>x</sub>	-11(13)		10	23(10)	+1.8(0.8)	+1(15)	
11	15(10)	+0.4(1.0) <sub>x</sub>	0(12)		16 03	08.9	x 17 53 30	(1,2)	1.14
12	14(11)	-2.0(1.3)	+16(20)				D155 (T118E)		
16 02	30.0	x 17 34 59	(1,2)	1.02	17	23(9)	0(0.6)	-2(9)	
		D30 (T108):			18	12(9)	-0.3(1.6) <sub>x</sub>	+12(18)	
11	59(16)	0(0.5) <sub>x</sub>	-10(7)	(38,0;20)	19	9(10)	-0.2(1.7)	+7(32)	
12	35(11)	0(0.4) <sub>x</sub>	+15(7)	(25,0;45)	16 02	53.1	x 17 53 31	(1,2)	1.04
13	13(12)	-0.5(1.6)	+27(26)				D82 (T112)		
16 02	15.1	x 17 36 16	(1,2)	1.09	12	17(9)	+0.9(0.9)	-9(14)	
		D31 (T98):			13	23(13)	-1.1(0.8) <sub>x</sub>	+3(13)	
4	33(10)	-0.4(0.5) <sub>x</sub>	-10(8)		14	22(11)	-1.0(1.1)	+1(12)	(47,0;80)
5	28(10)	0(0.6) <sub>x</sub>	+18(9)		16 02	55.4	x 17 53 36	(1,2)	1.04
6	14(11)	-1.3(1.3)	+11(18)				D81:		
16 03	00.2	x 17 40 28	(1)	1.10	16	25(15)	-0.5(1.0) <sub>x</sub>	+3(18)	
		D33:			17	13	-1.0(1.5) <sub>x</sub>	-2(25)	
1	17(10)	+0.7(1.1) <sub>x</sub>	-23(19)		16 03	45.3	x 17 53 55	(2)	2.11
2	24(12)	-0.2(1.1) <sub>x</sub>	-13(14)				OW245		
3	31(9)	-0.1(0.5)	+18(8)		4	68(27)	-0.1(0.5) <sub>x</sub>	+2(11)	

where  $a > 20''$  and  $F/\sigma_F > 2$ . We give these diameters mainly for comparison with future work, since the AIPS error estimates (plus the quadratic nature of deconvolution) suggest that size estimates are reliable only if  $a \gtrsim 40''$  and  $F/\sigma_F > 3$ . The entries in Table 1 show that this is satisfied in hardly any of the cases, i.e., with our present data we cannot give reliable sizes to the emission in individual channels.

In contrast to the pessimism of the last paragraph, we shall see in § IV that a "rotation signature" can be derived reliably from comparison between adjacent channels for a number of galaxies (position centers are more accurate than sizes for small sources). Contour plots for adjacent channels are compared for 15 galaxies in Figure 1. Single-channel contours are also shown

in Figure 1 for six galaxies as illustrations: for D60 and D80 the emission is strong ( $F/\sigma_F \gtrsim 4$ ), and the source is probably resolved; for OW 245, D155, and OW 251 the emission is strong enough ( $2 < F/\sigma_F < 3$ ) to give an accurate center but not resolution; the emission for D121 is below our acceptance threshold, and the whole feature may be spurious. Figure 2 gives channel contour plots for three larger regions containing a number of galaxies each. If a galaxy was observed in more than one field, all results in Table 1 (and Table 2) represent weighted means, but the contours in Figures 1 and 2 come from a single field each.

We also searched each of the three fields in each frequency channel for strong emission, not associated with any optical

TABLE 1—Continued

RA	x	Dec.	(Field)	GF	RA	x	Dec.	(Field)	GF		
Ch	$F(\sigma_F)$	$\Delta RA (\sigma_{RA})$	$\Delta Dec(\sigma)$	size (",";°)	Ch	$F(\sigma_F)$	$\Delta RA (\sigma_{RA})$	$\Delta Dec(\sigma)$	size (",";°)		
16	03	15.9	x 17 54 10	(1,2)	1.23	16	03	17.4	x 18 18 10	(3)	1.12
			D80 (T121):								
7	18(11)	-0.2(1.2)	x	-44(13)		24	14(12)	-0.4(1.3)	x	-14(22)	
8	42(11)	0(0.4)	x	-3(7)		25	12(11)	+1.4(1.3)	x	-i3(25)	
9	28(12)	-0.7(0.8)	x	+20(10)							
				(27;0;25)							
16	02	45.7	x 17 54 32	(1,2)	1.04	16	04	00.8	x 18 18 59	(3)	1.05
			OW133:								
1	18(14)	+0.3(1.0)	x	-2(20)		4	16(13)	+1.0(2.0)	x	+2(16)	
2	29(15)	-0.4(0.8)	x	-3(15)		5	24(12)	-0.3(0.8)	x	+14(12)	
3	14(12)	+0.6(1.3)	x	+4(21)							
16	03	27.0	x 17 56 03	(2)	1.47	16	04	02.8	x 18 19 02	(3)	1.05
			OW221:								
14	33(12)	+0.7(0.6)	x	+2(9)		7	12(8)	-0.2(1.0)	x	-5(20)	
15	24(12)	+0.5(0.8)	x	-4(14)							
16	03	22.1	x 17 56 10	(2)	1.39	16	03	46.1	x 18 19 74	(3)	1.03
			D78 (T126):								
12	33(13)	-1.0(0.7)	x	-1(11)		8	28(10)	+0.7(0.5)	x	+5(7)	
13	32(10)	-0.5(0.5)	x	+16(8)		9	22(12)	-0.9(1.0)	x	+4(14)	
14	35(12)	+1.5(0.6)	x	-6(7)							
15	23(11)	+1.5(0.8)	x	+1(10)		16	02	44.5	x 18 19 22	(3)	1.77
				(35,0;145)							
				(24,0;160)							
16	03	59.2	x 18 05 17	(3)	1.39						
			D100:								
[5]	10(10)	+1.2(2.0)	x	-9(29)		16	02	25(16)	+1.1(1.0)	x	-16(17)
6	40(10)	-0.3(0.4)	x	-1(6)							
7	21(19)	-1.2(1.6)	x	-11(16)		16	03	38.4	x 18 21 16	(3)	1.08
8	17(15)	-0.5(1.6)	x	-6(18)							
16	03	51.0	x 18 10 12	(3)	1.10	9	14(9)	-2.1(1.0)	x	+6(15)	
			D108:			10	35(10)	-2.1(0.4)	x	+10(6)	
2	15(13)	+1.2(1.5)	x	+15(21)		11	27(9)	-0.9(0.5)	x	-2(7)	
3	26(10)	0(0.6)	x	-1(8)		12	41(11)	+0.4(0.4)	x	-15(6)	
16	03	47.5	x 18 14 49	(3)	1.01	16	04	22.6	x 18 22 44	(3)	1.51
			D118 (T138):								
9	34(9)	0(0.5)	x	-6(6)		6	40(18)	+0.1(0.8)	x	+3(10)	
10	14(9)	-1.3(1.0)	x	-8(14)							
11	9(8)	-0.3(1.7)	x	-22(24)		16	03	22.6	x 18 24 27	(3)	1.45
16	03	51.4	x 18 17 20	(3)	1.01	6	18(11)	+0.7(1.0)	x	-24(10)	
			OW251:			7	32(11)	-0.1(0.6)	x	+8(8)	
6	11(8)	+1.2(1.2)	x	-3(20)							
7	21(10)	+0.3(0.8)	x	+4(11)		16	03	57.6	x 18 27 45	(3)	1.45
16	03	18.1	x 18 17 41	(3)	1.12	9	22(17)	-0.8(1.6)	x	-17(18)	
			D121 (T123):			10	35(17)	-0.4(0.7)	x	+11(14)	
[23]	20(15)	-0.1(1.6)	x	-16(12)							
						16	03	13.4	x 18 28 31	(3)	1.75
						5	49(14)	-0.8(0.5)	x	-10(7)	
						6	53(14)	+0.5(0.4)	x	-14(5)	

## Remarks on individual galaxies:

OW 166: the channel nine emission may be from the galaxy itself. The channel 10 emission is either noise or some kind of intergalactic cloud (see text).

D31/33: note the gap in declination, marking the border between A2151 S and C.

D156/155: there is no sign of spatial (nor velocity) distortion in either galaxy, in spite of their proximity on the sky. The two nearby galaxies D80 (NGC 6054) and D82 (NGC 6045) are quite separate on the VLA maps (see Fig. 2).

OW 221/D78: the small galaxy OW 221 and the large, peculiar D78 (IC 1182; see Bothun, Stauffer, and Schommer 1981) are mainly resolved, but have some hydrogen in common (see Figs. 1 and 2).

D78/D100: note the gap in declination, marking the border between A2151 C and N.

galaxy position. We found no obvious sources with  $F/\sigma_F$  appreciably above two (although a number with this ratio approaching two, e.g., one with  $F \approx 20$  mJy and  $\sigma_F \sim 11$  mJy near  $16^h02^m49^s \times 17^\circ35'5''$ ), but we did not search for weaker but extended sources. One possible very extended weak source (or collection of small, weak sources) was seen near the position of OW 166 (first item in Table 1, also shown in Fig. 2). Unfortunately our sensitivity is not sufficient to distinguish a large, low-density gas cloud from mere noise.

As discussed above, the quantity  $F$  in Table 2 (expressed in units of  $10^{-4}$  Jy) is meant to be the spatially integrated flux, but is likely to underestimate extended emission. For galaxies with individual channel emissions which satisfy the criteria for signal to noise and position given above we have summed the channel fluxes  $F$  to give the total intensity  $S$  and its probable error  $\sigma_s$ . In Table 2 we list all galaxies for which  $S/\sigma_s$  exceeds two as "detected" (and a few galaxies of special interest which do not satisfy this criterion) and the mean heliocentric velocity

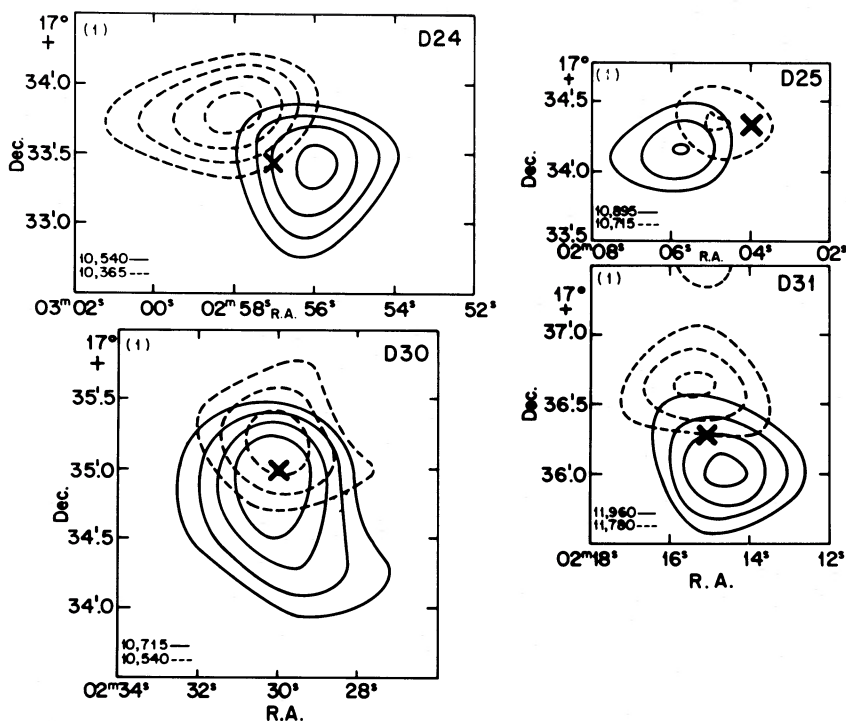


FIG. 1a

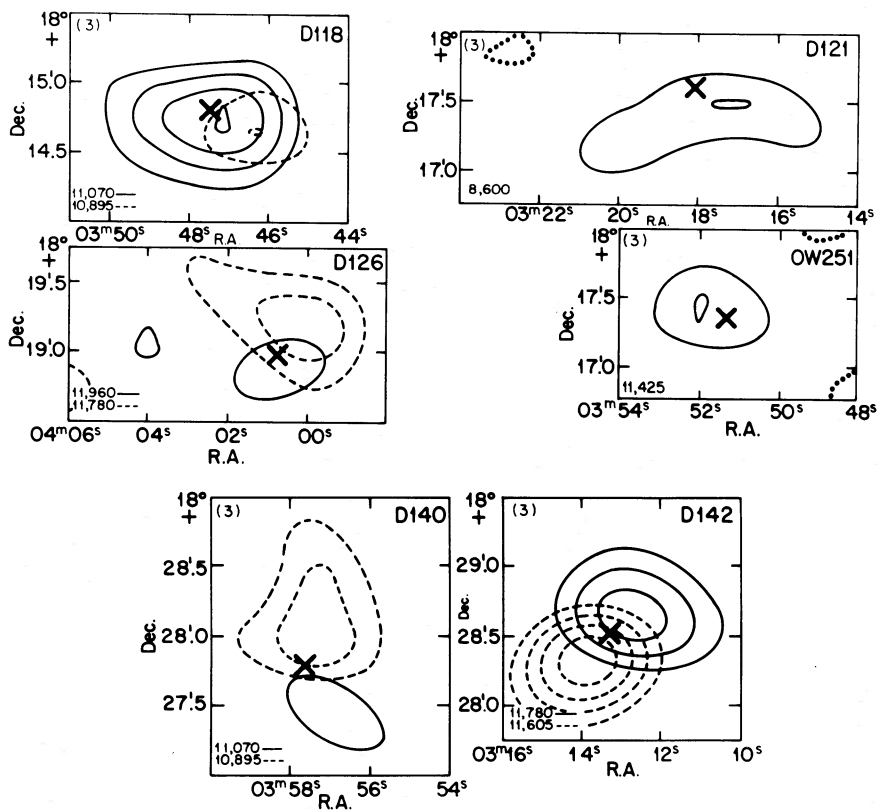


FIG. 1e

FIG. 1.—Flux contour maps for individual galaxies for either a single frequency channel or a pair of channels. When a pair of channels is displayed, negative flux contours are suppressed; for single-channel maps, negative contours are shown dotted. The field number is shown at the top left, velocities at bottom left, and the optical galaxy center is denoted by a cross. The contour levels are 0.9, 1.5, 2.1, and 2.7 mJy.



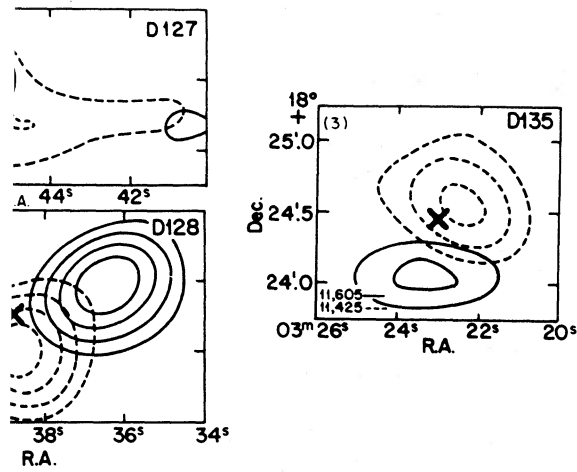


FIG. 1c

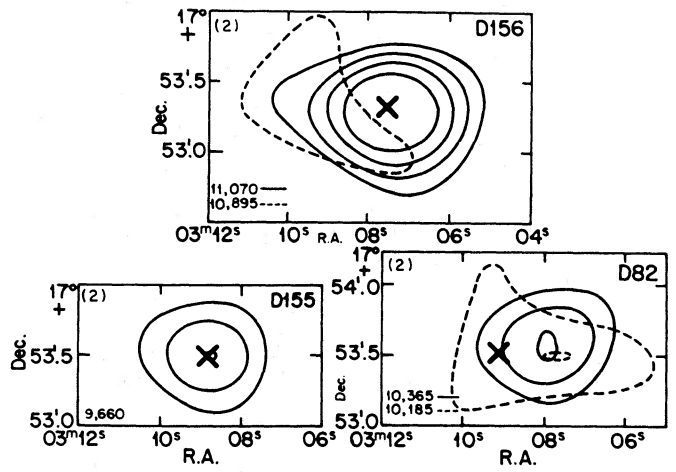


FIG. 1d

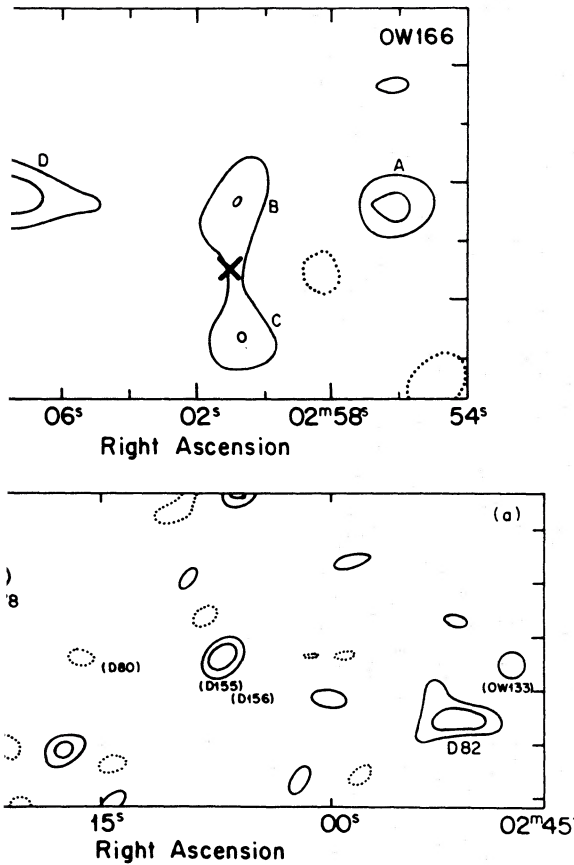
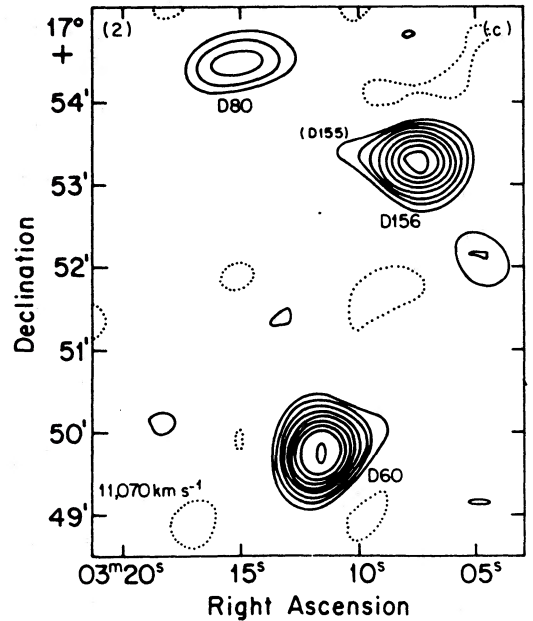
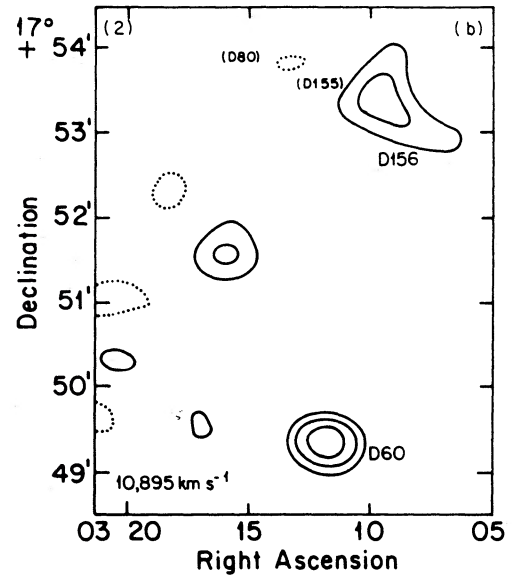


FIG. 2a

single channel (velocity marked in lower left) for some crowded larger areas (a, b, and c). Emission (or noise) peaks in the vicinity of the galaxy OW 166 are also marked. Emission (or noise) peaks in the vicinity of the galaxy OW 166 are also marked with +0.8, 1.2, 1.6, 2.0, 2.4, 2.8, 3.2, and 3.6 mJy for (a), (b), and (c); for OW 166



FIGS. 2b, 2c

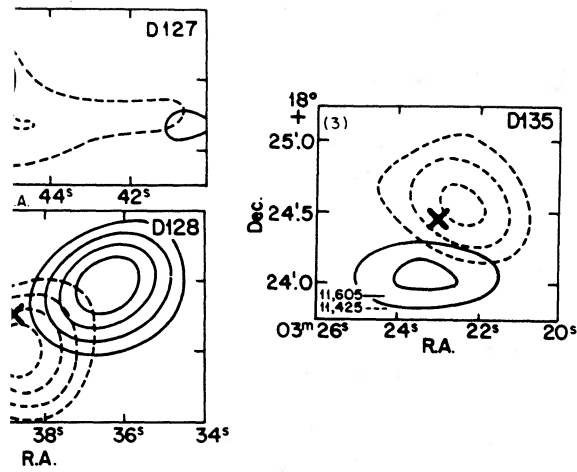


FIG. 1c

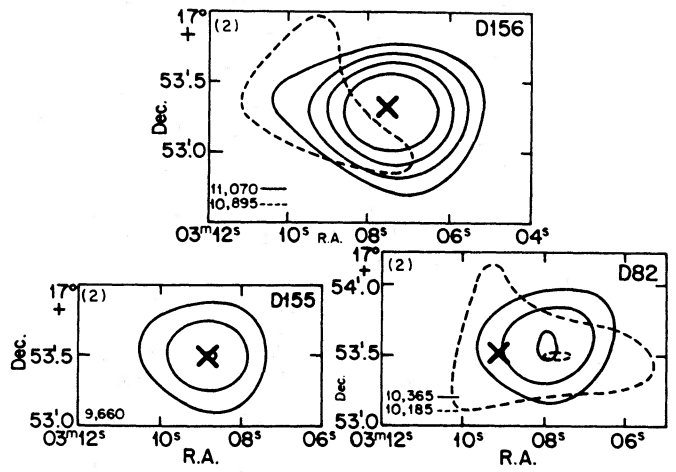


FIG. 1d

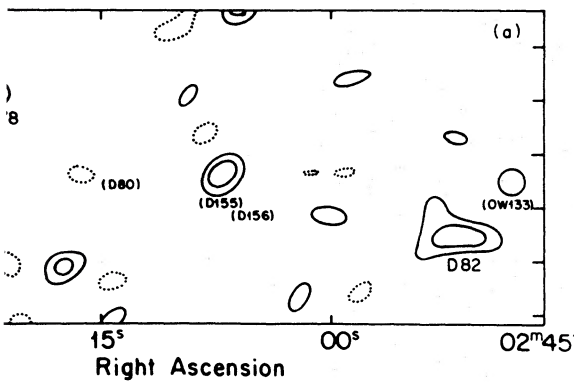
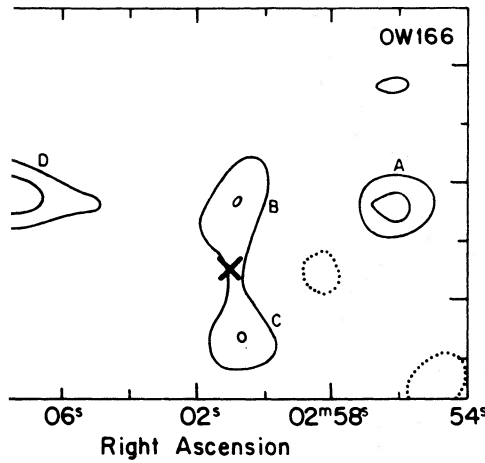
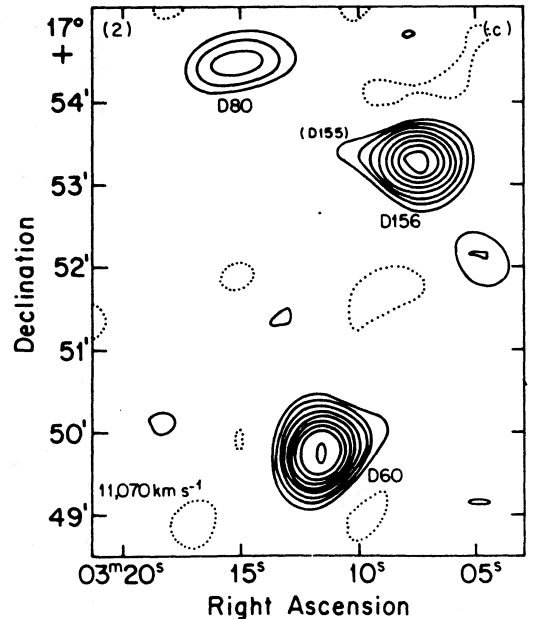
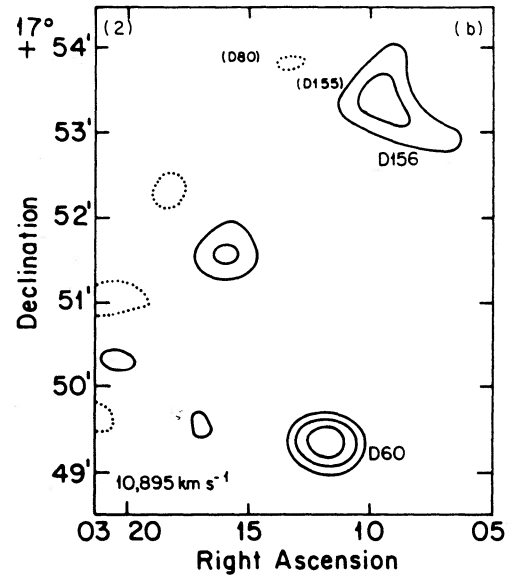


FIG. 2a

single channel (velocity marked in lower left for some crowded larger areas and c). Emission (or noise) peaks in the vicinity of the galaxy OW 166 are also +0.8, 1.2, 1.6, 2.0, 2.4, 2.8, 3.2, and 3.6 mJy for (a), (b), and (c); for OW 166



FIGS. 2b, 2c



TABLE 2  
OVERALL PROPERTIES OF DETECTED GALAXIES

D Number	Type (m.i.)	T Number	NGC/IC Number	$M_{\text{H}}(\sigma_{\text{H}})$ ( $\times 10^8 M_{\odot}$ )	Our $V_0$ ( $\text{km s}^{-1}$ )	Previous $V_0$ ( $\text{km s}^{-1}$ )	$W$ ( $\text{km s}^{-1}$ )	$D(\sigma_D)$	$\theta(\sigma_{\theta})$	$\theta_{\text{opt}}$
D18	Sc(16)	...	...	105(52)	10266	...	310	41''(38)	324''(38)	350*
D20	Sc(15)	...	...	92(27)	10610	...	310	...	...	...
D24	Sbc(14)	113	I1173	169(37)	10452	10439	460	47 (21)	235 (18)	220
D25	S(16)	...	...	84(30)	10804	...	415	47 (29)	114 (25)	100
D30	Sb(14)	108	...	179(38)	10610	10638	365	28 (13)	176 (19)	170
D31	Sc(15)	98	...	125(30)	11840	11889	365	29 (13)	12 (18)	0
D33	S(15)	...	...	120(30)	12263	...	420	42 (24)	165 (24)	155
D38	Sc(16)	...	...	94(28)	12206	...	295	28 (22)	125 (32)	...
D49	Sc(15)	...	...	37(17)	10186	...	135	...	...	...
D60	Sc(15)	...	U10190	192(28)	11080	...	355	56 (19)	349 (14)	350
[OW 181]	...	...	...	30(15)	8250	...	135	...	...	...
D156	Sc(15)	118W	I1179	144(25)	11040	11097	365	31 (16)	278 (21)	310
D155	Sbc(15)	118E	N6050	70(28)	9571	9598	270	...	...	...
D82	Sbc(13)	112	N6045	104(32)	10330	10049*	450	30 (24)	111 (32)	85
[D81]	S $\phi$ (16)	...	...	63(33)	9770	...	155	...	...	...
OW 245	...	...	...	114(45)	11959	...	135	...	...	...
D80	Sc(14)	121	N6054	147(33)	11225	11178	235	64 (18)	174 (12)	160*
OW 133	...	...	...	102(45)	12320	...	330	...	...	...
OW 221	...	...	...	94(28)	10110	...	275	...	...	...
D78	S $\phi$ p(14)	126	I1182	206(38)	10290	10091*	590	38 (15)	267 (16)	270
D100	Sc(15)	...	...	144(40)	11540	...	375	...	...	...
D108	Sb(15)	...	...	69(27)	12190	...	185	...	...	...
D118	Sb(15)	138	...	95(25)	11000	11022	290	...	...	...
[OW 189]	...	...	...	43(27)	8350	...	275	...	...	...
OW 251	...	...	...	53(22)	11479	...	255	...	...	...
D126	Sa(14)	144	I1189	67(30)	11855	11662*	255	...	...	...
[OW 271]	...	...	...	20(13)	11425	...	135	...	...	...
D127	Sbc(14)	139	...	84(27)	11175	11215	275	23 (20)	88 (35)	80
D128	Sb(13)	136	U01095	196(33)	10760	10722	545	41 (12)	300 (12)	290
OW 294	Sc?	...	...	65(30)	11603	...	135	...	...	...
D135	SBb(15)	127	...	94(28)	11470	11407	255	34 (20)	159 (24)	110
D140	S(16)	...	...	95(40)	10940	...	265	...	...	...
D142	Sc(15)	...	...	170(33)	11690	...	315	31 (13)	322 (17)	325

$V_0$  of the emission. For all galaxies with  $S/\sigma_s > 2$  the values of  $V_0$  fall between 9250 and 12,300  $\text{km s}^{-1}$ , whereas a noise spike could have fallen well outside this range, and very few (if any) of our 29 detections are likely to be spurious. The “detections” are much more dubious for the four galaxies (in brackets) in Table 2 with  $S/\sigma_s \leq 2$  (two of these might be foreground galaxies, and two lie close to other galaxies). We give in Table 2 our values of  $M'_{\text{H}}$ , the hydrogen mass for a nominal assumed distance of the Hercules cluster of 200 Mpc ( $H_0 = 55 \text{ km s}^{-1} \text{ Mpc}^{-1}$ ). With  $S$  in units of  $10^{-4}$  Jy times  $177 \text{ km s}^{-1}$ , the mean channel velocity width, we have  $M'_{\text{H}} \equiv M_{\text{H1}} (200 \text{ Mpc}/d)^2 = S \times 1.67 \times 10^8 M_{\odot}$ , where  $M_{\text{H1}}$  and  $d$  are the actual hydrogen mass and actual distance.

IV. COMPARISON WITH OPTICAL AND ARECIBO DATA

Most of our 31 claimed H I detections, and of our 16 claims to have resolved the principal axis of a rotation signature, are only slightly above the nominal detection threshold. We have also used additional selection criteria which refer to the known optical positions of the galaxies. The precise meaning of the internal error estimates of the AIPS fitting program is not clear in such cases, but we can make comparisons with Arecibo and optical data for an external check.

Thirteen of the detected galaxies in Table 2 are in the Zwicky catalog (T list), and of these all but one (D127, T139) has been observed successfully at Arecibo. For D78 (T126) we use for the Arecibo comparison the data in Schommer, Sullivan, and Bothun (1981); for the others we use the compilation by Giovanelli and Haynes (1984). Three of the galaxies (D82, 78, and

126) will be discussed below because of blending with a close companion, but for the remaining nine galaxies we can make direct comparisons to help improve error estimates for our various results. The systemic velocity  $V_0$  in our results minus the Arecibo value has a mean of only  $-5 \text{ km s}^{-1}$  and a dispersion  $\sigma$  of  $41 \text{ km s}^{-1}$ . The *a priori* error estimate for  $V_0$  for a strong and very narrow spectral line is the channel width divided by  $2\sqrt{3}$ , which is  $51 \text{ km s}^{-1}$  for our  $177 \text{ km s}^{-1}$  channels. The expected error could, of course, be larger if the spectrum is noisy, but is smaller if the signal covers many channels and is strong. Note that our definition for  $V_0$  is not the usual radio definition of “average between the two sloping edges of the spectrum” (which we cannot determine adequately because of our poor resolution) but corresponds to the “mean emission.”

The velocity width  $W$  is very poorly determined by our results because of our poor resolution, its definition is slightly arbitrary, and its evaluation is somewhat subjective—especially for a narrow line (for emission detected reliably in only a single channel we adopt a value of  $135 \text{ km s}^{-1}$ , about  $\frac{3}{4}$  the channel width) for  $W$ . Our mean  $W$  for the nine galaxies is only  $\sim 7 \text{ km s}^{-1}$  smaller than the Arecibo value (which was obtained with much better velocity resolution), and the dispersion of the difference between the two determinations is  $\sim 70 \text{ km s}^{-1}$ .

For five T galaxies there is an H I detection (or marginal detection) in Table 1 for another galaxy, separated by less than the Arecibo width of  $3/2$ , and for three of these the Arecibo spectrum is badly blended: (i) the optically faint S0 galaxy D81

lies 33" from the bright galaxy D82 (T112, NGC 6045) and shows moderately strong H I emission (Tables 1 and 2) with  $V_0 = 9770 \text{ km s}^{-1}$  and  $W \approx 160 \text{ km s}^{-1}$ , compared with  $V_0 = 10,330 \text{ km s}^{-1}$  and  $W = 450 \text{ km s}^{-1}$  for D82. The Arecibo emission spectrum for the two galaxies combined (Fig. 3 of GH) agrees well with our combined data in Table 1 and gives a (combined)  $V_0 = 10,049 \text{ km s}^{-1}$  and  $W = 660 \text{ km s}^{-1}$ . Although the separation of 33" is only comparable with the VLA resolution, and our (somewhat conservative) criteria assign only a marginal detection to D81 in Table 2, the positional errors in Table 1 are fairly small and the assignment to two separate galaxies is probably real. These two galaxies are in a crowded region of the cluster core (see our Fig. 2a), and the velocity separation of  $560 \text{ km s}^{-1}$  is large, so that an optical projection may be more likely than a physical pair. Unlike the Arecibo data (discussed by Bothun 1981), the VLA emission from D82 is not confused with that from D155/156. (ii) The faint galaxy OW 221 lies 70" from D78 (T126, IC 1182) and shows unequivocal emission (see our Tables 1 and 2 and Fig. 1) in two channels, which overlap with the lower frequency emission from D78. The Arecibo spectrum agrees moderately well with our combined spectrum, and there is little doubt in the assignment to the galaxy pair. This is likely to be a physical pair, discussed further in § VI. (iii) The faint galaxy OW 271 lies 29" from D126 (T144), and Table 1 shows emission in channel seven with  $F/\sigma = 1.5$ . The Arecibo spectrum (Fig. 3 of GH) again agrees with our combined spectrum; a VLA D-configuration positional error of 27" at  $F/\sigma_F = 1.5$  (which would be required to invalidate our assignment to two different galaxies) has moderately low probability. (iv) The galaxy D80 (T121, NGC 6054) is separated from D156 (T118W, IC 1179) by  $\sim 2.4$ , and the two systemic velocities are similar. The VLA not only separates these two galaxies, but each is somewhat resolved in Figure 2. The Arecibo data could suffer from blending, but the actual Arecibo assignments agree fairly well with the unambiguous VLA data. (v) The pair of bright galaxies D155 (T118E) and D156 (T118W, IC 1179) have a positional separation of only 21", but their velocities were known to be very different (see also § VI), and the Arecibo assignments for  $V_0$  and  $W$  agree with ours. For two T galaxies, D19 (T133) and D59 (T134), marginal detections at Arecibo are thrown in doubt by our failure to see any emission (D148, T146, also detected at Arecibo, is outside the reliable portion of our fields).

For the nine unambiguous detections in common between Arecibo and the VLA, we can compare values for the total intensity  $S$ . The ratio of the Arecibo value to our value has a mean of  $1.23 \pm 0.08$  and a dispersion of 0.24. The systematic difference of  $\sim 23\%$  is mainly due to two effects which tend to depress our VLA intensity values: (a) If the actual distribution of emission for a given channel has a concentrated core plus an extended halo, the AIPS Gaussian fit is likely to omit the halo; (b) our detection criterion not only has a signal-to-noise requirement but also a rather stringent requirement on the positional emission center relative to the optical galaxy position. Upward fluctuations in noise can lead to too large a positional error and the complete elimination of a weak channel from our sum for  $S$ .

For galaxies with reliable emission data in Table 1 for two or more channels, one can derive data on the "rotation signature" of the galaxy. In Table 2 we give values for the length  $D$  and principal axis angle  $\theta$  of the two-dimensional vector pointing from the center position of the lowest reliable channel in Table

1 (highest velocity) to that of the highest channel (lowest velocity). The values  $\theta = 0^\circ$  and  $180^\circ$  denote arrowheads pointing to positive and negative declination, respectively;  $\theta = 90^\circ$  and  $270^\circ$ , to positive and negative right ascension, respectively. The rms error  $\sigma_D$  in the "rotation diameter  $D$ " is derived from the AIPS error estimate for the individual positions. Our estimate  $\sigma_\theta$  for the rms error in the position angle is the small-angle approximation  $\sigma_\theta = (\sigma_D/D)$  (1 rad/ $\sqrt{2}$ ). We give values in Table 2 for all galaxies with  $\sigma_D < D$ . For each of these 15 galaxies we also give  $\theta_{\text{opt}}$ , our visual estimate for the position angle of the optical major diameter taken from the POSS plate. The quantity  $\theta_{\text{opt}}$  is defined modulo  $180^\circ$ , and we have chosen the value within  $180^\circ$  of the H I value of  $\theta$ . The rms of the difference between  $\theta$  and  $\theta_{\text{opt}}$  (which includes the considerable error in our visual estimate for  $\theta_{\text{opt}}$ ) is only  $19^\circ$ , compared with an rms of  $22^\circ$  for  $\sigma_\theta$  alone. This suggests that the standard AIPS error estimates we have used are overestimates for our data, possibly because of one of our selection criteria: we rejected any channel emission with position center more than  $35''$  from the optical galaxy center; some emissions with particularly large noise are thus missing entirely in Table 1.

Although the errors contributed by noise to the quantity  $D$  may be small, this quantity is only weakly related to any of the usual definitions for a "hydrogen diameter." Our definition for  $D$  would be inapplicable for a completely face-on galaxy, and in general it refers to positions of highest surface brightness for matter near the maximum rotation velocity and not to any scale length or isophotal positions. We shall call  $D$  the "hydrogen rotation diameter."

## V. H I CONTENT

As discussed in § IV we adopt D81 and OW 271 in Table 2 as detected, but omit OW 181 and OW 189 which are below our official threshold, leaving 31 detections. We do not have optical magnitudes for most of our galaxies, but we divide optical galaxies into "bright" (T), "medium-bright" (M), and "faint" (F) as follows: there are 20 "bright" Zwicky galaxies (T numbers in Table 2) classified as spirals (Sa or later). Of the 64 galaxies on the D list which are too faint to be on the T list, 48 are classified Sa or later and are denoted as M spirals. Of 140 galaxies on the OW list, too faint to be on the D list and not known to be E or S0, we do not have Hubble types for many, but we estimate that  $\sim 100$  are Sa or later—our F spirals. The ratio of mean luminosity is probably  $\sim 2\text{--}4$  each for T/M and M/F. We detected 13 of the 20 T spirals with a mean hydrogen mass (assuming a nominal distance of 200 Mpc) of  $\bar{M}_H = 15 \times 10^9 M_\odot$  per detected galaxy ( $\bar{M}_H > 10 \times 10^9 M_\odot$  per galaxy). We detected 12 of the 48 M spirals with  $\bar{M}_H = 10 \times 10^9 M_\odot$  per detection ( $\bar{M}_H > 2.6 \times 10^9 M_\odot$  per galaxy) and six of the 100 F spirals with  $M = 8.4 \times 10^9 M_\odot$  per detection ( $\bar{M}_H > 0.5 \times 10^9 M_\odot$  per galaxy). The ratio  $M_H/L$  must be impressively large for the six detected F galaxies, but we detect only a small fraction—both facts in part a reflection of our high detection threshold for  $M_H$ . There may be a tendency for hydrogen-rich faint galaxies to have low surface brightness, but this is not yet statistically significant: of the six detected F galaxies, OW 245, 251, and 294 have quite low surface brightness (especially OW 251), but OW 133 and 271 are bright and compact (OW 221 is interacting and peculiar, see § VI).

Accurate optical magnitudes are available for only a few of our galaxies (Bothun 1981), and our values for the velocity widths  $W$  are very crude. We therefore cannot make quantitative statements about any hydrogen deficiencies or the Tully-

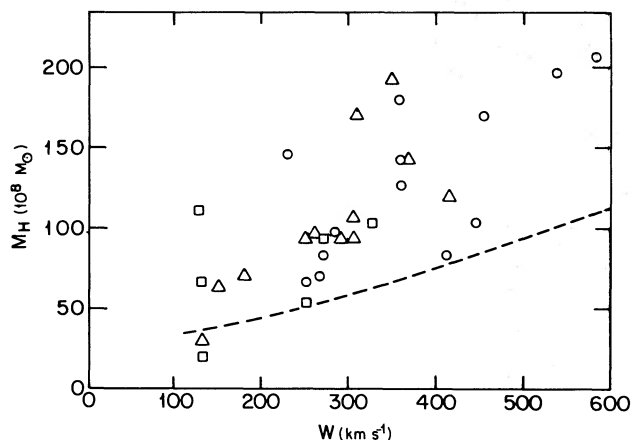


FIG. 3.—Hydrogen mass ( $M_H$ ) plotted against velocity width  $W$ . Squares refer to faint (F) galaxies, triangles to medium-bright (M), and circles to the bright galaxies of the T list. Dashed line is an approximate detection threshold.

Fisher relation. However, Figure 3 gives a plot of  $M_H$  versus  $W$  for detected galaxies, separately for T, M, and F galaxies—at least in qualitative agreement with the usual positive  $M_H$ - $W$ - $L$  correlation.

As described in § III, very few of the single-channel H I maps have a large enough emission size and good enough signal to noise to give a reliable H I diameter. However, the center positions for single-channel emissions are reliable enough that we see a “rotation signature” for 16 of the 31 detected galaxies. As described in § IV, the principal axes  $\theta$  for these 16 galaxies agree well with the optical principal axes  $\theta_{opt}$ , modulo  $180^\circ$ . However,  $\theta$  is a uniquely defined angle between  $0^\circ$  and  $360^\circ$ , since we measure which end of the major diameter has the larger velocity, and we can test for any preferred rotation orientation. We find  $\langle \cos \theta \rangle = +0.06 \pm 0.18$  and  $\langle \sin \theta \rangle = -0.04 \pm 0.18$ ; i.e., there is no detectable preferred orientation for rotation. None of the eight detected galaxies with  $M_H < 0.8 \times 10^{10} M_\odot$  gave a reliable rotation signature; Figure 4 plots the “hydrogen rotation diameter”  $D$  against  $M_H$  for the remaining 23 detections and shows no clear-cut correlation,

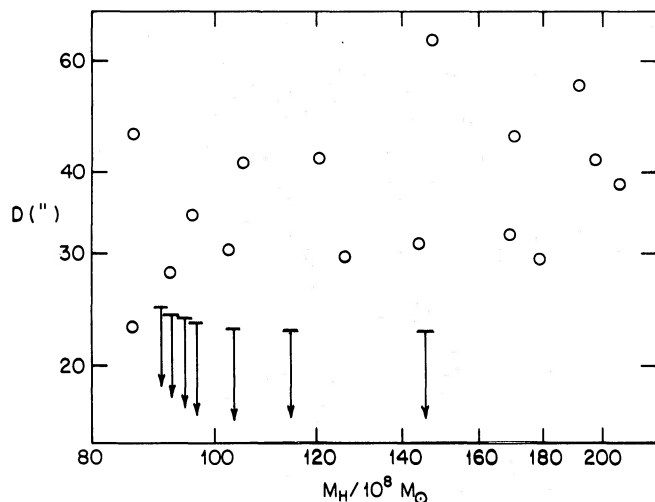


FIG. 4.—Hydrogen rotation diameters  $D$  plotted against hydrogen mass  $M_H$  for 16 resolved galaxies. Upper limits are indicated for seven other galaxies.

partly because this quantity is not tightly coupled with the overall H I diameter, as we discussed in § IV.

#### VI. THE PECULIAR GALAXY IC 1182

Bothun, Stauffer, and Schommer (1981) have discussed in detail previous work on the interesting galaxy IC 1182 (also called Mrk 298, D78, T126, and OW 200), which has magnitude  $B_0^T \approx 15.0$  and resides in the central portion of the Hercules cluster core A2151C (see our Fig. 2a). Its integrated color and optical morphology suggest an elliptical or S0 classification, but of a peculiar type. The unusual optical features include nuclear activity, somewhat similar to Seyfert galaxies, and a long, knotty jet extending eastward  $\sim 55''$  ( $\sim 75$  kpc at our assumed nominal distance of 200 Mpc). Figure 2 of Bothun, Stauffer, and Schommer (1981) shows an Arecibo spectral profile of IC 1182 and its surroundings, obtained with a beamwidth of  $\sim 200''$  FWHP. The H I emission has a full velocity width of  $W \approx 650$  km s $^{-1}$  and has two unusual features: (a) a large hydrogen mass  $M_H$  for an early-type galaxy and (b) a narrow “spike” near  $V_0 = 10,050$ – $10,100$  km s $^{-1}$  superposed on a flatter spectrum from  $\sim 9950$ – $10,600$  km s $^{-1}$ . Based on the optical peculiarities and the large hydrogen mass, Bothun, Stauffer, and Schommer (1981) had conjectured that IC 1182 has suffered a collision with some late-type (originally hydrogen-rich) galaxy in the recent past.

Our VLA data confirm the involvement of a second galaxy, the optically faint galaxy OW 221 (without any Hubble type assignment at the moment)  $\sim 73''$  eastward of IC 1182: the VLA maps (our Fig. 1 and Table 1) show that the main body of IC 1182 contains  $\sim 70\%$  of the total hydrogen mass of the combined system. The remaining 30% comes from OW 221 and from a weaker “hydrogen bridge” between the two galaxies. The “spike” in the Arecibo spectrum near  $V \approx 10,100$  km s $^{-1}$  (our channels 14 and 15 at 10,187 and 10,010 km s $^{-1}$ ) contains all of the H I of OW 221 and about half the H I of IC 1182, i.e.,  $\sim 65\%$  of the total. Thus, the systemic velocity of OW 221 seems to be close to the lower velocity of IC 1182’s rotation curve, which explains the asymmetry of the Arecibo spectrum (which includes the entire system).

Figure 1 of Bothun, Stauffer, and Schommer (1981) contains the optical image of IC 1182 and (near one edge) that of OW 221. The prominent, long optical jet starting at IC 1182 points moderately accurately, but not precisely, in the direction of OW 221. Furthermore, OW 221 shows a much shorter “jet” (or at least “elongation”) which points roughly in the direction of IC 1182. These two near coincidences in direction fully corroborate the dynamical involvement of this pair of galaxies.

*A priori* conjectures on collisions between galaxies in a crowded cluster core usually concentrate on unbound pairs on a chance collision course. Given the high velocity dispersion in A2151C, our observed velocity difference between IC 1182 and OW 221 is surprisingly small. Two possibilities are (i) an unbound pair with larger velocity difference mainly perpendicular to the line of sight or (ii) a bound pair with modest orbital velocity, whose orbit might have been perturbed by other members of the crowded core. We do not have an optical velocity for OW 221, and one might also raise the possibility that the H I we associate with this galaxy is only a plume raised by it, rather than orbiting gas. The small values of  $\Delta R.A.$  and  $\Delta \text{Decl}$  in our Table 1 (see also our Fig. 1) make this very unlikely. In each of two separate velocity channels the center of the H I emission is very close to the optical center of OW 221.

We also have VLA radio continuum data, derived from the

same observations by Dickey and Salpeter (1984). We found no continuum source associated with OW 221, but our source No. 27 (a previously known weak source) has its central position within  $3''$  of the optical nucleus of IC 1182. It is interesting to note that this source has an extended halo, but our sensitivity was insufficient to give any details on this extension. Young *et al.* (1984) have already pointed out that IC 1182 is the only prominent early-type galaxy in the Hercules cluster with emission in the far-infrared. *IRAS* data from more distant galaxies (Soifer *et al.* 1984) have already suggested a correlation between intense far-infrared emission and interacting galaxy pairs; the pair IC 1182-OW 221 adds to this suggestion.

#### VII. MORPHOLOGY AND DYNAMICS OF THE CLUSTER

Tarengi *et al.* (1980) discussed the structure of the whole Hercules supercluster before the optical data by Dressler (1980) and the radio data were available. The new data invite a rediscussion, at least for A2151.

For the core of A2151, which is elongated in the N-S direction, Tarengi *et al.* (1980) noted a velocity gradient and a "clumpiness" in the galaxy distribution. With the data then available they suggested that the core may consist of two separated subcores, but there is more complexity in the new

data: Geller and Beers (1982) have analyzed the surface number density distribution from the D list and still find "clumpiness" in A2151, but now *at least* three "lumps" are required (S, C and N, roughly corresponding to our three VLA fields, shown in Fig. 3). The distribution and physical nature of radio continuum sources in A2151 (Dickey and Salpeter 1984) also suggests the presence of three "plasma clumps." Three dynamically distinct subcores for the Hercules cluster is then one possibility, but "general clumpiness" in a single dynamic unit is another. The complexity of Geller and Beers's contour plots and the displacement between the southern "plasma clump" and southern concentration of bright optical galaxies slightly favor the latter. Fortunately, we have more dynamical information from systemic velocities.

We have H I values for the systemic velocities for the 31 galaxies in our Table 2 and the Arecibo value  $V_0 = 11,128 \text{ km s}^{-1}$  for D148 (T146). In addition we have optical data for 23 Zwicky galaxies (see Tarengi *et al.* 1979; Giovanelli and Haynes 1984), which were not detected in H I. Nondetection for these bright galaxies implies a small value for  $M_H/L$ , which is of particular interest for the seven spirals in this group: T88, T96N, T129, T133, T134, T135, and T149. Approximate values for the heliocentric velocities  $V_0$  are shown in Figure 5. Accurate

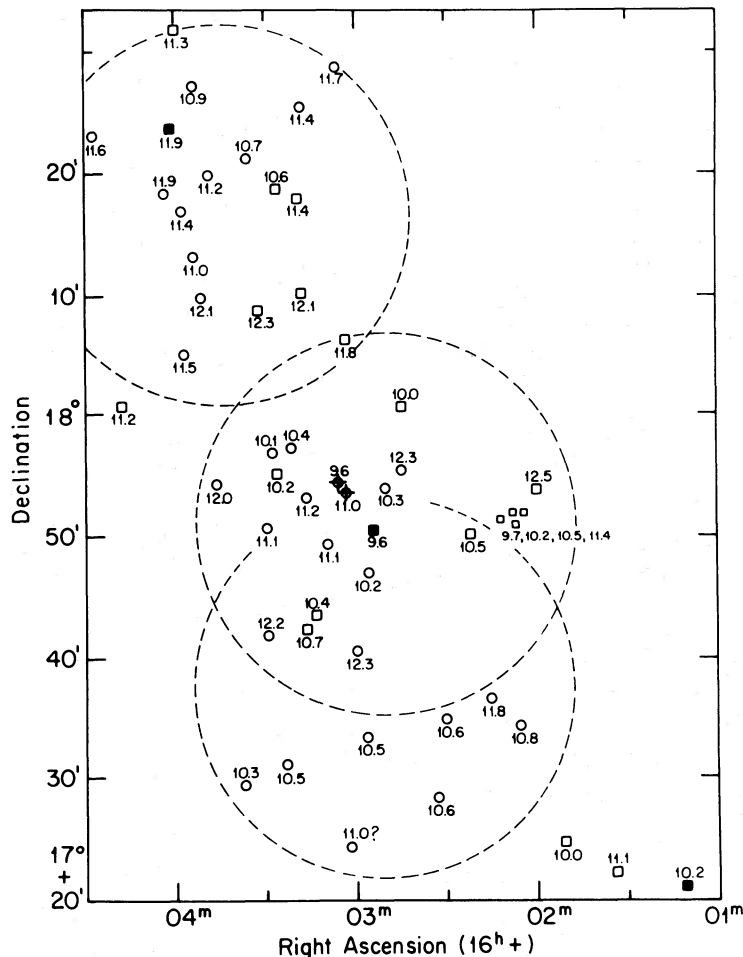


FIG. 5.—Systemic velocities (heliocentric), in units of  $100 \text{ km s}^{-1}$  for galaxies in the three VLA fields in the Hercules cluster. Dashed circles show where the primary beam gain is half the peak value ( $GF = 2$ ). Circles denote VLA H I detections (plus an Arecibo detection for D148); squares denote optical velocities. The three strong radio-continuum emitters are indicated by solid squares; the interesting "pair" D155/156 by crossed circles.

TABLE 3  
MEAN ( $\bar{V}$ ) AND VARIANCE ( $\sigma$ ) OF (HELIOCENTRIC) SYSTEMIC VELOCITIES  
FOR VARIOUS GROUPS

Group	Number	$\bar{V}$ (km s <sup>-1</sup> )	$\sigma$ (km s <sup>-1</sup> )
S, all .....	9	10622 ± 191	574
C, detected .....	13	10952 ± 273	986
C, undetected .....	13	10570 ± 275	991
N, detected .....	13	11400 ± 111	399
N, undetected .....	7	11423 ± 228	602
Spirals .....	39	11142 ± 126	784
E and S0 .....	16	10506 ± 206	825
Undetected spirals .....	7	11466 ± 307	811
All .....	55	10957 ± 114	841

velocity means  $\bar{V}$  and dispersions  $\sigma$  are given in Table 3 for various combinations of location and of individual galaxy properties.

Separating the south (S) from the center (C) at declination anywhere between 17°37' and 17°40', C from N anywhere between 17°57' and 18°05', we get the results in the first five lines of Table 3. For C and N we have enough galaxies to also separate H I detected from undetected galaxies, and two conclusions are uncontroversial: irrespective of H I content, (a) mean velocities are largest in the north, and (b) the velocity dispersion is appreciably larger in the center than in either S or N. A detailed inspection of the individual galaxies in Figure 5 shows no sign of any discontinuity in velocity, as would be expected if one were dealing with two or three independent dynamic units. Furthermore, some of the smallest velocities occur in the northern half of the center (9600 km s<sup>-1</sup> for T118E), and some of the largest occur in the southern half of the center (12,300 km s<sup>-1</sup> for D33). Empirically and theoretically, a single dynamic group or cluster tends to have velocity dispersion decreasing outward; this is satisfied here if we are dealing with a single, elongated cluster but violated for two (or three) separate clusters. We return to the small velocity gradient in § VIII. This picture of A2151 as a single dynamical unit is further supported by an analysis of unpublished optical galaxy velocities (Bothun 1984, private communication) which show a smooth velocity distribution.

Tarengi *et al.* (1980) noted the possibility of some dynamic differences between elliptical and spiral galaxies, but the H I data have made this question more controversial rather than less: a division into hydrogen-rich (detected) versus hydrogen-poor (undetected) is similar to a division into spirals versus E + S0, except that the seven undetected spirals trade places. In the top half of Table 3 we find no significant difference in mean velocities between detected and undetected galaxies, but in the bottom half we find that the spirals have a larger mean velocity than the ellipticals by an amount of 2.6 times the expected rms difference. This curious difference in the differences stems from the seven undetected spirals which have a particularly large mean velocity. It is not clear whether we are dealing with a statistical fluctuation or some subtle physical effect. At a given location, there is no significant difference in velocity dispersion  $\sigma$  between detected, undetected, spiral, or elliptical galaxies; this reinforces the significance of the decrease in  $\sigma$  with increasing distance from the cluster center.

### VIII. DISCUSSION

The main results of our VLA observations of the extended core of the Hercules cluster (A2151) are the detection of 31 galaxies and the mapping of a rotation signature for 16 of

these. We comment first on the significance for observational technique: compared with Arecibo (single-dish) observations of the same or similar galaxies, our VLA observations had only a slight edge in sensitivity, but the advantages of (i) much better angular resolution and (ii) being able to observe optically faint (or invisible) objects and the disadvantage of (iii) much poorer velocity resolution. For most of the galaxies for which we claim a detection, the signal-to-noise ratio was precariously close to the nominal detection threshold, but we gave arguments which suggest that the nominal error estimates are somewhat pessimistic. Resolving some galaxies and detecting some faint ones with the VLA alone was gratifying, but we also feel that joint VLA-Arecibo observations are important for some purposes: Arecibo can measure velocity widths  $W$  with great precision, but there is fear of including emission from a companion galaxy in the spectrum. We have found evidence for three such pairs in A2151 where the Arecibo observations alone would give too large a value for  $W$ . The galaxy pair IC 1182-OW 221 provides a particularly interesting case of an interacting pair. Conversely, however, for those bright galaxies where we have *not* found a close-by companion with the VLA we now know that the Arecibo widths are reliable. We hope to apply this technique to a few other clusters.

Although many redshifts were known for the Hercules supercluster as a whole, we have added significantly to the data base on systemic galaxy velocities for the relatively small core of A2151. We feel it is most likely that this core, although elongated and "clumpy," is a single dynamic unit with velocity dispersion decreasing with radial distance from the center—as is the case for a number of other clusters. There is a relatively small velocity gradient from south to north, which could be due to a small rotational component or merely some velocity shear. The rotational velocity gradient along the major axis of an individual galaxy is *not* correlated with any direction in the sky (neither parallel nor perpendicular to the cluster's south-north gradient), but only some extreme models for galaxy formation predict such correlations.

The situation is not clear regarding any dynamic differences between spiral and elliptical galaxies for A2151: unlike spirals in the Virgo cluster, the spirals here do *not* have significantly larger velocity dispersions than the ellipticals, and the spatial distributions are not very different. We have the marginally significant feature of seven undetected spirals having a particularly large mean velocity. If this were a physically significant effect, one would expect the hydrogen-poorer detected galaxies to have a slightly larger mean velocity than the richer galaxies, but this is *not* the case: considering only detected galaxies, those with  $M_H < \bar{M}_H$  have  $\bar{V} \approx 10,987$  km s<sup>-1</sup>, those with  $M_H > \bar{M}_H$  have  $\bar{V} \approx 11,222$  km s<sup>-1</sup>.

The use of the VLA or similar aperture synthesis telescopes for observations of 21 cm H I emission from spirals in rich clusters like Hercules has great potential for further work. Clearly at the distance of Hercules Arecibo's tremendous advantage in sensitivity is beginning to be cancelled by its lower resolution. In many cases confusion among two or three galaxies all contained in the Arecibo beam has caused problems for the interpretation of spectra from that telescope. For more distant clusters this problem will be much more severe. At the distance of Hercules the VLA resolution even in D-array is sufficient to separate galaxies, and somewhat resolve many. Unfortunately, clusters at distances much larger than Hercules will be difficult to synthesize with the present VLA system because the signals will be so weak. Even with 36 hr of integra-

tion (12 per field), this study is hampered by low signal-to-noise ratios for the fainter galaxies. The best hope for studies of more distant clusters is either an improvement of the system temperatures of the VLA 21 cm receivers, or perhaps the embellishment of Arecibo with several outlying antennas similar to the Los Canos dish (Kulkarni *et al.* 1985).

We are particularly indebted to Drs. Okamura and Wakamatsu for providing us with their list of galaxies with accurate positions, which was extremely helpful in the analysis of our

data, and to Drs. G. Bothun, R. Giovanelli, and M. Haynes for private communications. We are also grateful to Drs. A. Dressler, M. Geller, G. Helou, J. Huchra, and J. van Gorkom for interesting discussions and suggestions, and to Cyndi Jordan for help with the data analysis. This work was supported in part by NSF grants AST 84-15162 to Cornell University and AST 82-16879 to the University of Minnesota, and by a grant from the Graduate School, University of Minnesota. J. D. acknowledges support from a fellowship from the Sloan Foundation.

## REFERENCES

- Bothun, G. D. 1981, Ph.D. thesis, University of Washington.  
 Bothun, G. D., Stauffer, J. R., and Schommer, R. A. 1981, *Ap. J.*, **247**, 42.  
 ———. 1985, in preparation.  
 Dickey, J. M., and Salpeter, E. E. 1984, *Ap. J.*, **284**, 461.  
 Dressler, A. 1980, *Ap. J. Suppl.*, **42**, 565.  
 Geller, M. J., and Beers, T. C. 1982, *Pub. A.S.P.*, **94**, 421.  
 Giovanelli, R., Chincarini, G. L., and Haynes, M. P. 1981, *Ap. J.*, **247**, 383.  
 Giovanelli, R., and Haynes, M. P. 1984, NAIC Rept., No. 200.  
 Hjellming, R. M. 1983, *An Introduction to the NRAO VLA* (Socorro: NRAO).  
 Kulkarni, S. R., Turner, K. C., Heiles, C., and Dickey, J. M. 1985, *Ap. J. Suppl.*, **57**, in press.  
 Okamura, S., and Wakamatsu, K. 1983, unpublished.  
 Schommer, R. A., Sullivan, W. T., and Bothun, G. D. 1981, *A.J.*, **86**, 943.  
 Soifer, B. T., *et al.* 1984, *Ap. J. (Letters)*, **278**, L71.  
 Tarengi, M., Tift, W., Chincarini, G., Rood, H., and Thompson, L. 1979, *Ap. J.*, **234**, 793.  
 ———. 1980, *Ap. J.*, **235**, 724.  
 van Gorkom, J. 1983, in *Synthesis Mapping*, ed. Thompson and D'Addario (Socorro: NRAO), p. 1.  
 Young, E., Soifer, B., Low, F., Neugebauer, G., Rowan-Robinson, M., Miley, G., Clegg, P., de Jong, T., and Gautier, T. 1984, *Ap. J. (Letters)*, **278**, L75.

JOHN M. DICKEY: Department of Astronomy, 116 Church St. SE, University of Minnesota, Minneapolis, MN 55455

EDWIN E. SALPETER: Center for Radiophysics and Space Research, 424 Space Science Building, Cornell University, Ithaca, NY 14853